HIGH PERFORMANCE TRANSLUCENT SOFT PIEZOELECTRIC NANOCOMPOSITES

by

Shichen Xu

An essay submitted to the Johns Hopkins University in conformity with the requirement for the degree of Master of Science

Baltimore, Maryland

December 2019

Abstract

Soft piezoelectric nanocomposites have attracted significant interest due to their flexibility and stretchability which are beneficial for a variety of applications. However, there is no soft and transparent piezoelectric material with good piezoelectric performance

The transparency of piezoelectric nanocomposite would be beneficial for the applications that need both good transmission of light and energy harvesting/sensing capability. To address this issue, a facile method to fabricate high performance soft piezoelectric nanocomposites with enhanced light transmission is developed by incorporating silver nanowires as conductive fillers.

During the fabrication process, ethanol was used to help the mixing of the composites and continuous magnetic stirring was applied during ethanol evaporation for good blending of the composite. After curing the mixture, the piezoelectric coefficient (d_{33}) was measured to evaluate the piezoelectric performance by measuring the electric output as a function of a mechanical loading. The data analysis showed that the silver nanowire incorporated piezoelectric

composite has a higher d_{33} coefficient (d_{33}~100 pC/N at its peak) than that of the commercially available PVDF (d_{33}: 30~40 pC/N).

We envision that the methods we developed and the findings from the study will contribute to applications of piezoelectric composites for a wider range of applications and provide guidelines for future research.

Primary reader and advisor: Prof. Sung Hoon Kang

Secondary reader: Prof. Chen Li

Acknowledgments

I am very grateful to my research advisor, Professor Sung Hoon Kang, for his enlightening guidance, unfailing support and invaluable suggestions throughout the process of my research work and the essay.

I also owe my gratitude to all the group members who work with Professor Kang for their timely assistance and impeccable coorperation.

Dedication

This essay is dedicated to my parents and parents-in-law,

Weiqing Gao and Peixi Xu, Yan Han and Yun Zhong for their eternal support.

And to my beloved wife, Ziyan Zhong and my unborn daughter for the bliss and inspiration they brought to my life.

Contents

Abstract ii

Acknowledgments iv

Dedication v

List of tables ix

List of figures x

Chapter 1 1

Introduction 1

1.1 Piezoelectric composites 1

1.1.1 Piezoelectric effect 1

1.1.2 Piezoelectric materials 3

1.1.3 Piezoelectric polymers and composites 4

1.1.4 Fabrication of piezoelectric composites 6

1.1.5 Performance of piezoelectric composites 8

1.2 Introduction of silver nanowires 9

1.3 Incorporation of silver nanowires with polymer composites 10

1.4 Transparency of piezoelectric composites 12

1.5 Applications 13

1.5.1 Robotics 13

1.5.2 Monitoring and diagnosis 16

1.6 Outline of the essay 17

Chapter 2 18

Sample preparation 18

2.1 Fabrication preparation 18

2.1.1 Experiment design and materials 18

2.1.2 Controlled environmental conditions 19

2.2 Fabrication process 20

2.3 Key variables and conditions 23

2.4 Chapter conclusion 24

Chapter 3 25

Test and Result discussion 25

3.1 d_{33} test and piezoelectric output 25

3.2 Percolation analysis of silver nanowire network 32

3.4 Chapter conclusion 34

Chapter 4 36

Conclusion and future work 36

4.1 Conclusion 36

4.2 Future work 37

Bibliography 38

Vita 44

List of tables

1	Comparison of properties of several conductive nano electrodes	12
2	Comparison of different types of actuation mechanisms of microrobotic devices	16
3	Loading test for d_{33} coefficient measurement	28
4	Standard deviation (STD) and average d_{33} values for each testing sample	30
5	Average d_{33} comparison between piezo nanocomposite and PVDF	30

List of figures

1.1	Schematic representation of different piezoelectric effects	2
1.2	Classification of piezoelectric polymers	4
1.3	Flexible nanocomposite-based generator made of $BaTiO_3$ NPs and graphitic carbons	6
1.4	$BaTiO_3$ nanoparticles with MW-CNT NCG	7
1.5	Schematic of d_{33} coefficient	8
1.6	SEM image of the PVP-capped Ag nanowires in large quantity	9
1.7	A representative SEM image of the sections of thus-obtained Ag nanowires	10

1.8	Polymer embedding process applied to the AgNWs films	11
1.9	MinRAR V1 prototype robot and leg configuration	14
1.10	MinRAR V1 prototype robot and leg configuration	14
1.11	Fully released m-DoF leg	15
1.12	Schematic drawing of actuation substructures	15
1.13	Output voltage, and power of the harvester resulted from the movements of the chest	17
2.1	Mixing of silver nanowires and $BaTiO_3$ nanoparticles	21
2.2	Liquid composite molding process	22
2.3	Fully cured piezoelectric nanocomposite	23
3.1	d_{33} measuring platform	26
3.2	Shaker setup	26
3.3	LabVIEW user interface	27

3.4	Sample prepared for testing	27
3.5	d33 coefficient of all testing groups under 2.5 N~ 7.5 N loading condition	29
3.6	Electric charge generated from all testing group	31
3.7	Measurement data from a previous study by Jeong et al. showing the generated outputs from periodic stretching/releasing of piezoelectric composites	31
3.8	Plot of sheet resistance versus volume of Ag nanowire solution	34

Chapter 1

Introduction

1.1 Piezoelectric composites

1.1.1 Piezoelectric effect

The word *Piezoelectricity* is originated from Greek and means "electricity from pressure". Electric charges will appear when certain material (such as crystals and certain ceramics) is subjected to mechanical stress from different directions.[1] The piezoelectric effect is also a reversible process as shown in Fig 1.1. The material which exhibits the piezoelectric effect can generate certain mechanical strain resulting from an applied electric field.

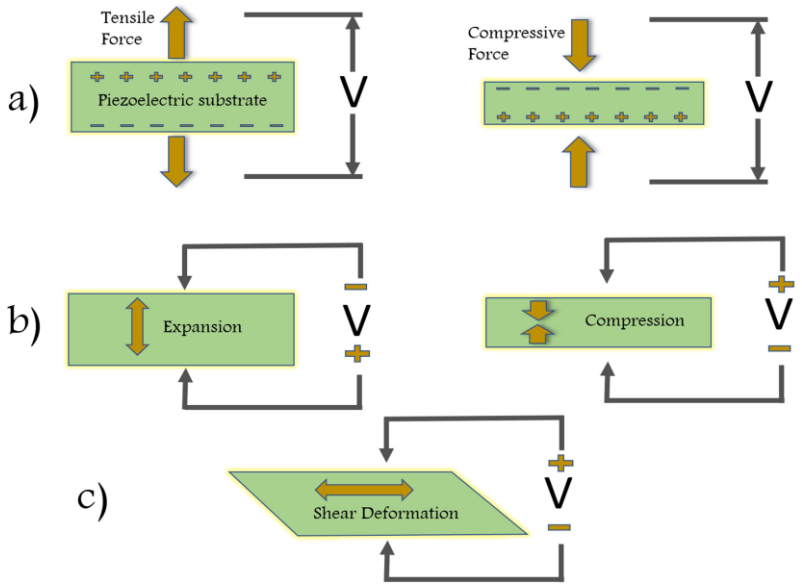

Fig 1.1 Schematic representation of different piezoelectric effects; reproduced with permission from [7] © 2015 Royal Society of Chemistry

For example, a crystal can generate piezoelectricity when its structure is under mechanical deformation. In converse, the crystal can generate deformation due to an applied electric field.[2][3] The application of the piezoelectric effect has been introduced since early 20th century for military purpose such as low-frequency ambient vibration detector, which is made of piezoelectric ceramic, equipped on the submarines for scavenging signals.[36] The development of piezoelectricity and piezoelectric effect have come through a long way that is widely used in our everyday life such as quartz watches and cigarette lighters.

1.1.2 Piezoelectric materials

There is a wide range of piezoelectric materials either natural or synthetic. The materials that were first demonstrated the piezoelectric effect by Curie Brothers include quartz, topaz and tourmaline. These are natural materials that can generate charges under deformation.[1] Another well-known class of a piezoelectric material is a synthetic piezoelectric ceramic such as Barium titanate ($BaTiO_3$) and Lead zirconate titanate (PZT). The most common applications for the piezoelectric ceramics are to make ultrasonic transducers and piezoelectric resonators.[4] Another majority category of piezoelectric materials is piezoelectric polymers. Among all these polymers, there are three types of polymers as shown in Fig 1.2 that classified as bulk polymers, voided charged polymers and polymer composites.[5] Although the polymers cannot generate as much piezoelectric output as ceramics, they still hold the properties that ceramics cannot match such as flexibility, biocompatibility and biodegradability.[6]

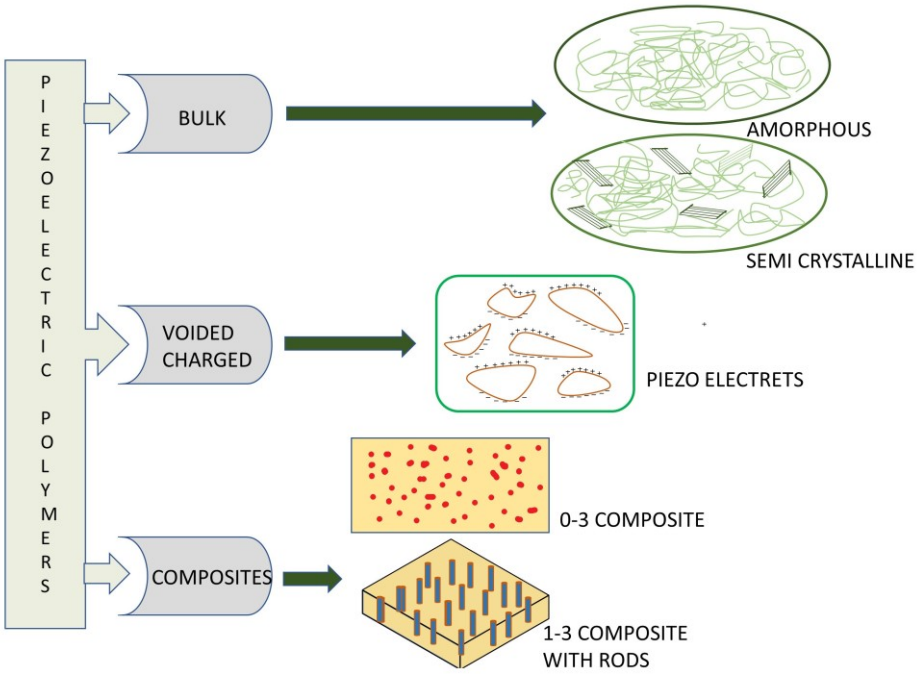

Fig 1.2 Classification of piezoelectric polymers; reproduced with permission from [7] © 2015 Royal Society of Chemistry

1.1.3 Piezoelectric polymers and composites

With the natural limitation of brittleness of piezoelectric ceramics, piezoelectric polymers such as PVDF, P (VDF-TrFE), poly propylene (PP) have been extensively explored for many applications since the 1950s. The piezoelectricity of these polymers is defined by their crystallinity. Polyvinylidenefloride (PVDF) is a special polymer which has many crystalline forms in which ß-phase creates a high piezoelectric effect.[7] Moreover, the piezoelectric effect can be detected in this group of composites by integrating piezoelectric ceramic particles into a polymer matrix. The matrix, in fact, does not have to be piezo-active to be an effective material.[8] The mechanical

property of polymer enables such composites to be flexible and wearable that traditional piezoelectric materials won't be able to accomplish.[9] The prevailing components of piezoelectric composites are categorized into three elements, which are matrix, piezoelectric filler and conductive additive. Polydimethylsiloxane (PDMS) is the most commonly used silicone rubber matrix material due to its low acoustic impedance, great chemical stability and low Young's modulus that can be easily prepared with readily accessible laboratory techniques.[10] Piezoelectric ceramic particles such as $BaTiO_3$, PZT, PMN-PT, ZnO which are of micro and nano dimensions are employed in polymer nanocomposites as piezoelectric filler candidates.[7] When it comes to nanocomposite, "nano" always refers to the scale of both piezoelectric particles and conductive filler. Fig 1.3 shows an example of $BaTiO_3$ based nanogenerator. The conductive additives serve as the conductor to provide better energy transitivity generated by the piezoelectric particles. Carbon nanotubes (CNT) and silver nanowires are both candidates as conductive fillers.

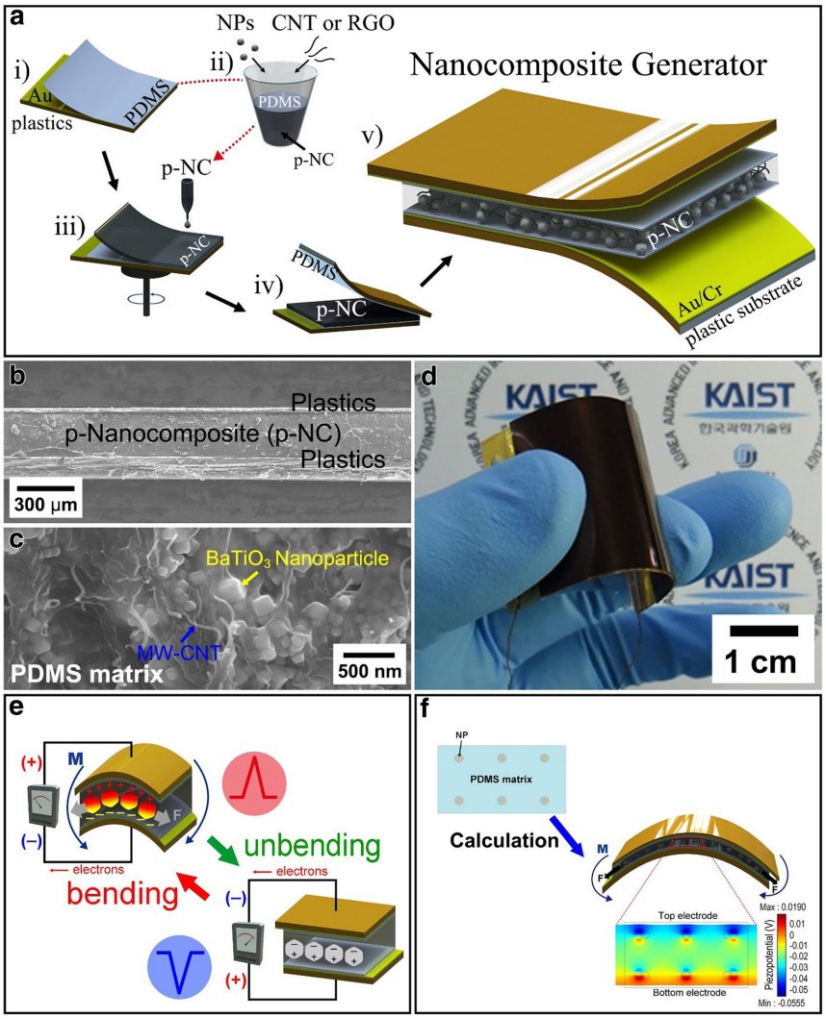

Fig 1.3 Flexible nanocomposite-based generator made of $BaTiO_3$ NPs and graphitic carbons. **a.** Schematic illustration showing the fabrication process of an NCG device by simple, low-cost, and scalable spin-casting. **b.** A cross-sectional SEM image of an NCG device. **c.** The magnified photograph of piezoelectric nanocomposite. **d.** The fabricated NCG device composed of p-NC and electrode-coated plastic substrates. e Schematics showing power generation mechanism of the NCG device. f Simulation model of an NCG device consisted of six $BaTiO_3$ NPs inside PDMS matrix and the calculated piezoelectric potential inside the p-NC method; reproduced with permission from [18] © 2016 Springer

1.1.4 Fabrication of piezoelectric composites

When it comes to the fabrication methods of piezoelectric composites, there are many that researchers have explored and validated such as thin-film material

deposition [11] and as simple as blending [7]. Piezocomposites can be made by blending piezoelectric ceramic particles and polymers as shown in Fig 1.4, but the connectivity patterns of these constituents control the electric flux pattern as well as the mechanical properties.[12] Such methods of fabricating piezoelectric composites are low-cost and easy to prepare in most research laboratories. In this essay, a similar methodology of fabricating translucent soft piezoelectric nanocomposites is illustrated with the focus of high piezoelectric output.

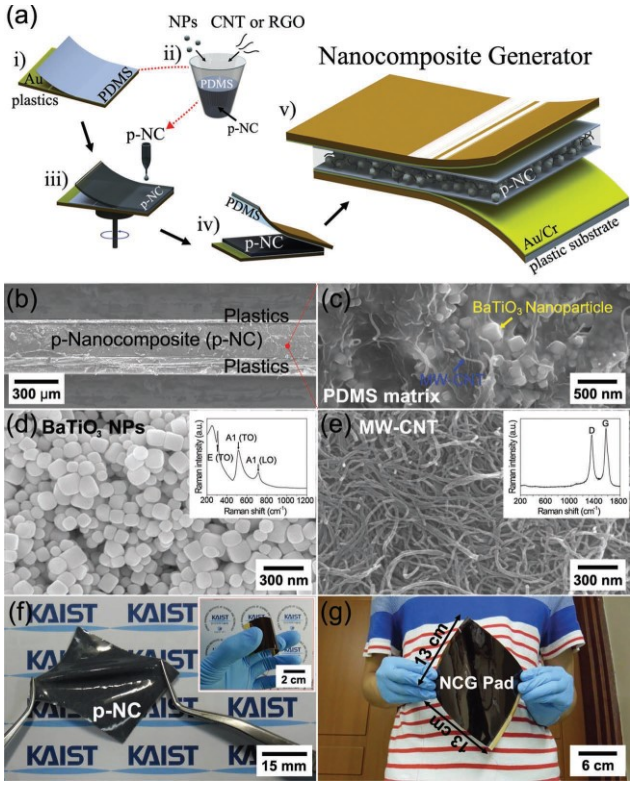

Fig 1.4 $BaTiO_3$ nanoparticles with MW-CNT NCG (a) Schematic illustration of the process for fabricating NCG device. (b) A cross-sectional SEM image of an NCG device. (c) A magnified cross-sectional SEM photograph of the p-NC. (d) A SEM image of the $BaTiO_3$ NPs synthesized by hydrothermal method. The inset shows a Raman spectrum obtained from and $BaTiO_3$ NPs. (e) The MW-CNTs have a diameter of 20 nm and a length of 2 μm. The inset shows a typical Raman shift of the MW-CNTs with large D bands. (f) Photograph of the p-NC stretched by tweezers. The inset shows the NCG device (3 cm x 4 cm) bent by fingers. (g) A large-area type NCG device (13 cm x 13 cm) fabricated by spin-casting or Mylar bar-coating.; reproduced with permission from [19] © 2012 WILEY-VCH Verlag GmbH & Co. KGaA, Weinheim

1.1.5 Performance of piezoelectric composites

Because the matrix of piezoelectric composite is made of viscoelastic materials, both elastic and viscous characteristics of the matrix would contribute to the piezoelectric response. Recent studies show a strong correlation between the piezoelectric output and the matrix polymer.[13] As shown in Fig 1.5, the hyper-stretchable nanocomposite generator utilizes its polymer matrix to maximize the piezoelectric output. With the study of solid mechanics, piezoelectric coefficient (d_{ij}) is used to quantify the direct piezoelectric effect, and it is expressed as $d_{ij} = D_i/\sigma_j$ (D_i is the electric displacement and σ_j is the applied stress).[14] The subscripts "$_i$" and "$_j$" indicate the directions of the induced electrical field and the mechanical loading, respectively. For example, as shown in Fig 1.5, d_{33} is for the situation when the electric field and the mechanical loading are both along the polarization axis ("3" direction).[13]

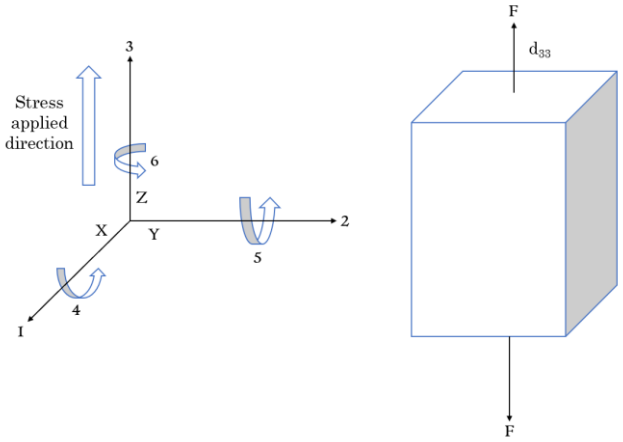

Fig 1.5 Schematic of d_{33} coefficient

1.2 Introduction of silver nanowires

Metallic nanostructures have drawn vast attention in applications such as nanoelectronics and transparent conductors.[15] In particular, one-dimensional metal nanowires are capable of providing devices and materials with novel functionality.[16] Unlike other nanostructures such as ZnO nanowires and Carbon Nanotube, silver nanowire possesses very high flexibility and conductivity at the same time. They are widely used for transparent transducers and transistors, as shown in Fig 1.6 and Fig 1.7 for their high carrier mobilities, the prospect of processing at low temperatures compatible with plastic substrates, as well as their optical transparency and mechanical flexibility.[17]

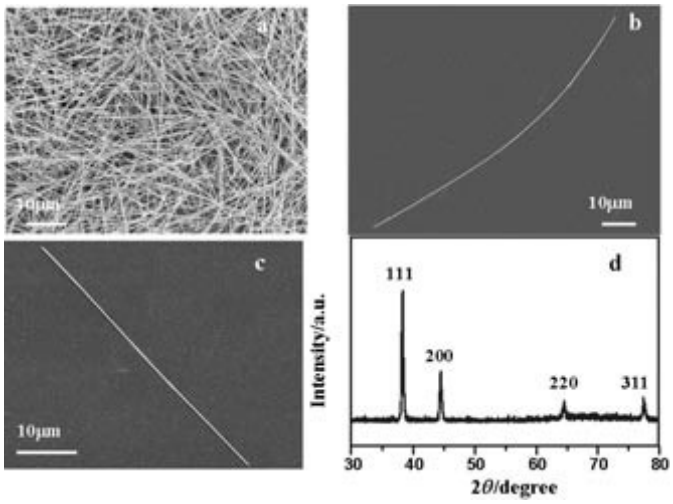

Fig 1.6 SEM image of the PVP-capped Ag nanowires in large quantity; reproduced with permission from [21] © 2004 WILEY-VCH Verlag GmbH & Co. KGaA, Weinheim

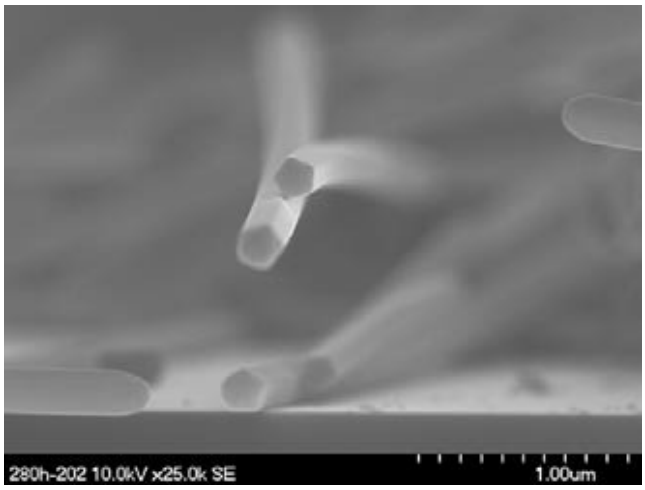

Fig 1.7 A representative SEM image of the sections of thus-obtained Ag nanowires: reproduced with permission from [21] © 2004 WILEY-VCH Verlag GmbH & Co. KGaA, Weinheim

1.3 Incorporation of silver nanowires with polymer composites

The incorporation of silver nanowires with polymer composites has been studied by many researchers for flexible electronics applications such as nanogenerators. An example of embedding silver nanowire with polymers is shown in Fig 1.8. Due to its outstanding conductivity and flexibility, silver nanowires are often implemented as a mesh network. The mechanical power-generating device called triboelectric nanogenerator (TENGs) is a perfect example of the application of silver nanowires.[22]

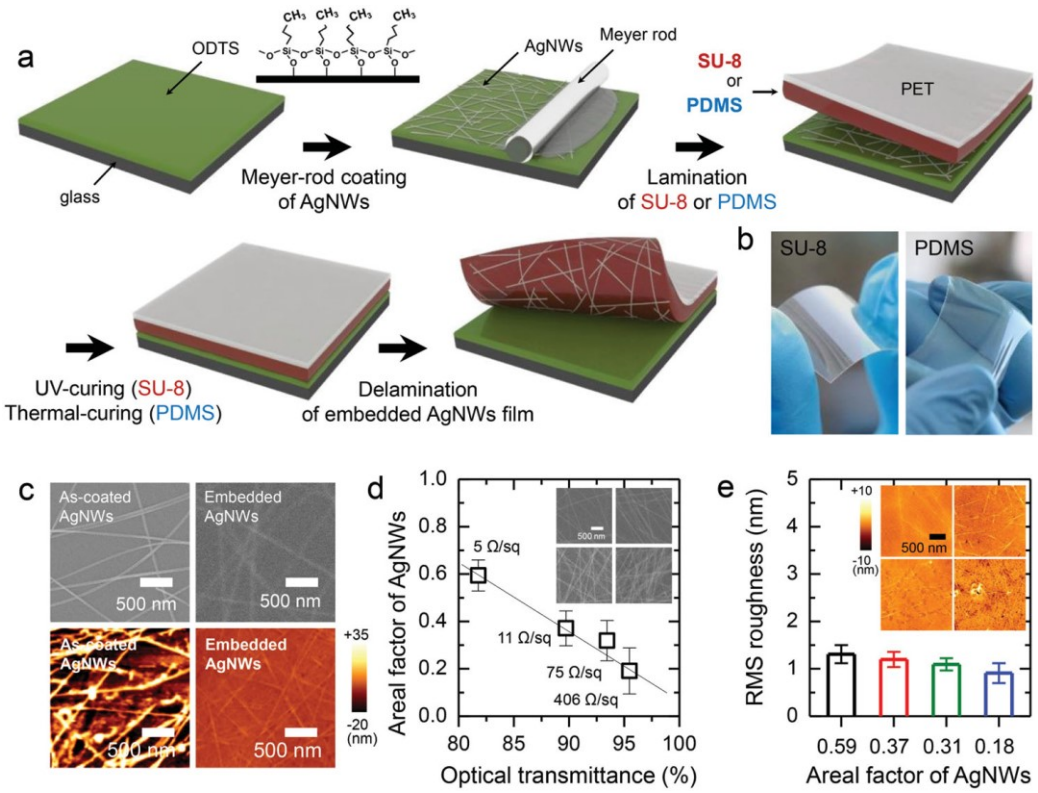

Fig 1.8 Polymer embedding process applied to the AgNWs films. a) Schematic diagram illustrating the polymer embedding process applied to the AgNWs films in this study. b) Optical images of flexible AgNWs embedded in SU8 mounted on a plastic substrate (PET), or stretchable AgNWs embedded in PDMS. c) SEM images (upper) and AFM topography images (lower) of AgNWs films based on as-coated AgNWs networks on glass or AgNWs embedded in films, for comparison. d) Areal fractions of AgNWs exposed to the surface, optical transmittances, and sheet resistances of the AgNWs films. The inset shows SEM images of AgNWs films (with four different sheet resistances) embedded in SU8. e) RMS roughness of the AgNWs films embedded in SU8. The inset shows the AFM topography images obtained from all samples.; reproduced with permission from [22] © 2016 WILEY-VCH Verlag GmbH & Co. KGaA, Weinheim

The stretchability of sliver nanowires contributes significantly to the mechanically induced electricity output of the composites, which out-races other composites filler candidate such as Carbon nanotube. Detailed comparison in each category with other materials are listed in Table 1. The "+" sign means above average properties and "—" means under average properties.

Table 1. Comparison of properties of several conductive nano electrodes; reproduced with permission from [23] © 2019 MDPI

Performance	ITO	Ag NWs	CNT	Graphene	Ag Nano Network
Sheet resistance	—	—	++	++	——
Transmittance	++	+	+++	++	+++
Stability	++	+++	++	++	+++
Flexibility	——	+++	+++	+++	—
Large scale	——	++	++	++	——
Fabricating cost	+++	—	++	+++	+++

Compared with common piezoelectric composites with Carbon nanotubes (CNT) filler, silver nanowires (Ag NWs) combined with Ag Nano Network have unbeatable advantages over CNT.[19] One key point is the property of transparency.[23] In this essay, the thin film silver nanowire blended piezoelectric composites will be fabricated and investigated based on its performance.

1.4 Transparency of piezoelectric composites

Not only do portable electronics create a huge demand of display technologies, but the need for medical diagnosis also draws great attention for the application of transparent sensors. The advantage of actively transferring mechanical deformation to electric output can be brought into many applications such as pneumonia diagnosis.

To achieve detectable electric output, the piezoelectric generator must reach certain level density. As a result, here comes the tradeoff between the transparency and the piezoelectric output. The transparency can provide the user with identifiable features during the procedure that will help improve the outcome of the diagnosis. While on the other hand, the good piezoelectric output is the key factor that the signal generated by the mechanical deformation can be accurately detected. The ideal piezoelectric material must be with the functionality of perform both transparency as well as high piezoelectricity output. In this essay, one method of fabricating translucent piezoelectric nanocomposite is presented toward the fully transparent piezoelectric materials.

1.5 Applications

To investigate into applications of piezoelectric nanocomposites, the mechanism that is being utilized needs to be fully understood. The piezoelectric capability allows the composite to generate electric charge while subject to mechanical deformation and vice versa. Based on this fact, signals and data can be collected by piezoelectric composites and actuators can be deployed with all kinds of configurations and structures. Many applications in either robotics or diagnosis have been explored by researchers as summarized in following sections.

1.5.1 Robotics

In recent studies, various kinds of small actuators are developed in the field of robot technology in applications of search-and-rescue and environmental monitoring.

The advantages of piezoelectric materials such as precision control and minimal energy consumption are ideal features that meet the need of miniature robots.[30] Ideal actuators would have larg e force or torque, long strokes at reasonable speed and high responsibility with precise positioning. Piezoelectric actuators almost satisfy all of these requirements.[31] The study of piezoelectric benders, which adopt soft piezoelectric materials, is gaining its attraction through recent years.

A prototype miniature resonant ambulatory robot (Fig 1.10) that uses piezoelectric actuators to achieve locomotion has been designed and fabricated. Each leg is comprised of two piezoelectric bimorph benders, joined at the tip by a flexure and end effector.[32]

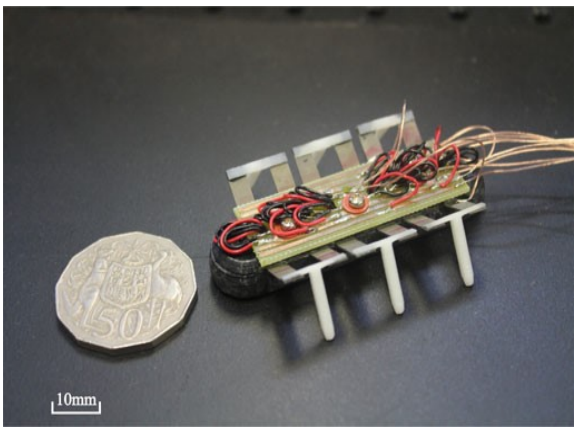

MinRAR V1 prototype robot

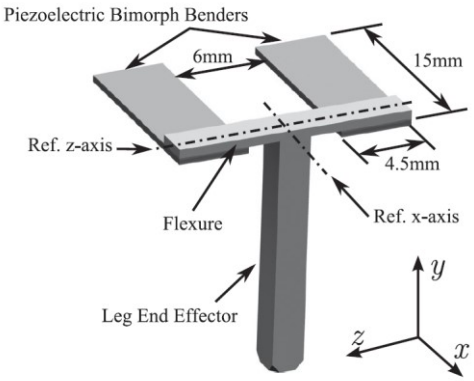

Leg configuration

Fig 1.9&1.10 MinRAR V1 prototype robot and leg configuration; reproduced with permission from [32] © 2016 IEEE

Another state-of-art design of microrobotic locomotion system is also reported in recent literatures as shown in Fig 1.12 and Fig 1.13 using a piezoelectric thin-film to achieve multi degree of freedom actuation. In this paper, thin-film lead zirconate

titanate (PZT) array is used as the piezoelectric force generator for the in-plane and out-of-plane motion of the microrobot.[33]

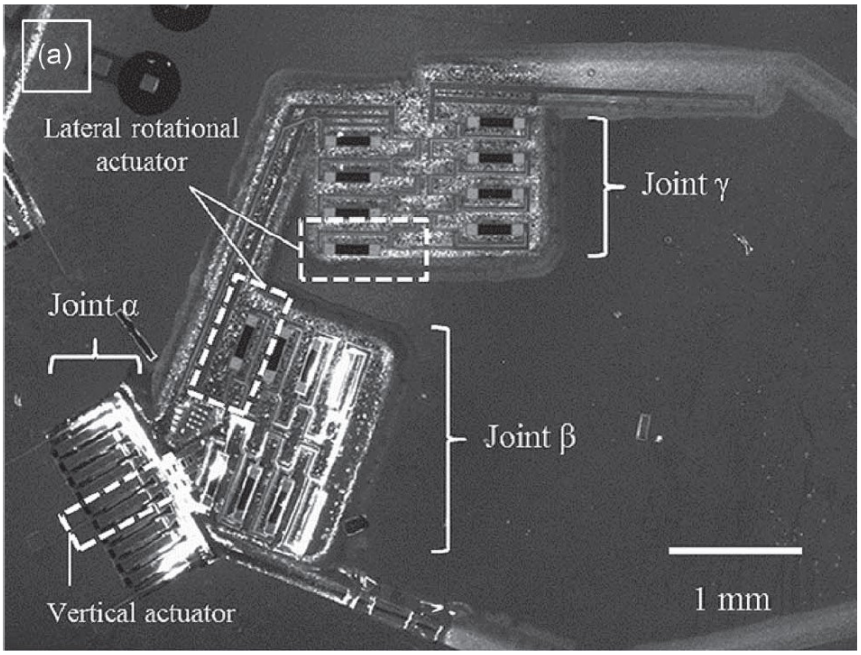

Fig 1.11 Fully released m-DoF leg; reproduced with permission from [33] © 2012 IEEE

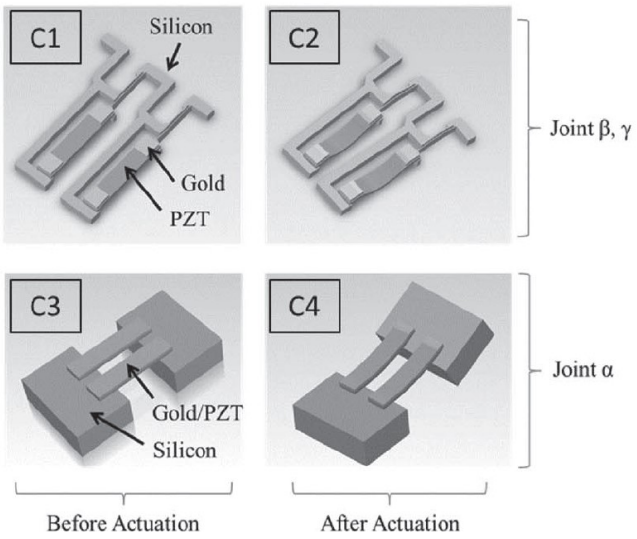

Fig 1.12 Schematic drawing of actuation substructures; reproduced with permission from [33] © 2012 IEEE

According the Table 2, the piezoelectric device outperforms other types of devices on speed, degree of freedom, maximum angle and power consumption in the field of microrobotic device. Although the subject in the table is piezoceramics which is not the same as piezoelectric composites, it still shows some advantages of piezo capability.

Table 2. Comparison of different types of actuation mechanisms of microrobotic devices; reproduced with permission from [33] © 2012 IEEE

	Weight Bearing	Speed [mm/s]	DoF	Maximum Angle	Volt	Power Consumption
Ebefors (Thermal)	312.5 mg/leg	6	1	~18.7°	18V	1.1W
Hollar (Electrostatic)	5.1 mg/leg	4	1	35°	50V	100nW
Murthy (Thermal)	667 mg/leg	1.55	1	~2.9°	10V	750mW
Mohebbi (Thermal)	1448 mg	0.64	3	N.A.	60V	Not specified
Current Work (Piezoelectric)	2.1 mg/leg	27 (est. max.)	3	5°, 40°	18V	60μW

1.5.2 Monitoring and diagnosis

Another significant contribution of piezoelectric soft composites make is the field of health monitoring and diagnosis. Regarding its property of ultra-sensitive to mechanical deformation, physical signals can be transmitted and harvested as electrical signals by the piezoelectric composites.

In recently published literature, the same output signal can be recorded as a physiological signal containing information about breathing, thus enabling piezoelectric self-powered wearable biosensors/harvesters. The empirical data obtained from testing different modules can provide evidence that such piezoelectric composite is applicable for detecting respiratory effort. Fig 13. shows a sample output

voltage (a), and power (b) of the sensor/harvester during normal breathing. The maximum peak voltage and maximum power are about 0.5 V, and 3 mW, respectively.[34]

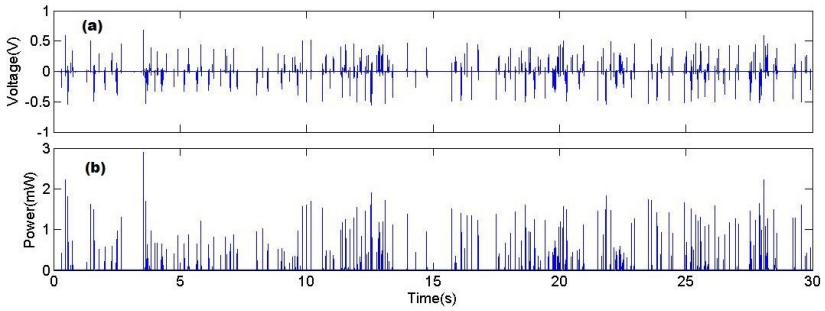

Fig 1.13 Output voltage, and power of the harvester resulted from the movements of the chest; reproduced with permission from [34] © 2013 IEEE

1.6 Outline of the essay

The structure of this essay is arranged as follows:

Chapter 2 will introduce the system setup and the fabrication process of the translucent silver nanowires piezoelectric nanocomposites.

Chapter 3 will lay out the testing method and results and analysis of piezoelectric nanocomposites.

Chapter 4 will discuss about conclusions and future work of the essay.

Chapter 2

Sample preparation

2.1 Fabrication preparation

2.1.1 Experiment design and materials

The method of the fabricating the piezoelectric composite is homogenously mixing each component with designated chemicals. To accommodate the need of evenly mixed composite, $BaTiO_3$ particles and the silver nanowires must be fully dispersed and blended with uncured PDMS base. Uncured composite mixture must be maintained a smooth and continuous stirring process instead of using a shaker. To achieve the goal, we adopted and modified the method from a previous study on fabricating piezoresistive composites.[24] The mixing ratio of $BaTiO_3$ particles, PDMS and silver nanowires is determined by the percolation threshold of silver nanowire network which will be discussed and analyzed in the results and discussion section.

Certain standard laboratory equipment is employed such as beakers, weighing trays, balance, pipette dropper, magnetic stirring bars and petri dishes. The most important equipment during the experiment is a stirring hotplate (Cimarec+TM) which provides continuous stirring and heating during evaporation.

Material wise, the commercial silver nanowire (Sigma-Aldrich, diam. × L 120-150 nm × 20-50 µm, 0.5% (isopropyl alcohol suspension)) is used to provide pure and robust network and consistent nanowire length since lab synthesized silver nanowires prone to vary from nanoparticles to small segments. As the piezoelectricity generator, the $BaTiO_3$ (US Research Nanomaterials, Inc., 99.9%, 300 nm, Tetragonal) is adopted due to its high output property whose d_{33} is reported to be 160 pC/N under room temperature.[35] PDMS base (SYLGARD® 184) and curing agent (crosslinker) are used as the polymer matrix for the soft piezoelectric nanocomposite.

2.1.2 Controlled environmental conditions

The experiment is conducted under the room temperature at 22 ℃. No specific humidity is required while preparing and mixing chemicals. The dispersing of $BaTiO_3$ nanoparticles, silver nanowires and the evaporation of ethanol from PDMS are all conducted inside the fume hood with air ventilation. Overnight experiment is expected due to the long evaporation process with the heated magnetic stirring process. All the glass beakers are prewashed and rinsed, and isopropanol is recommended for final rinsing.

2.2 Fabrication process

To ensure the functionality of fabricated sample, simple calculation of the amount of each chemical has been performed. The majority portion of weight is contributed by the PDMS base and curing agent. Based on the availability of beakers in the lab, the 50 mL size beaker with good condition and cleanliness is chosen to be the container of mixing process. Approximately 20 g of sample is expected due to the safety and capacity of beaker and unattended processes with the hotplate. The general mixing ratio of PDMS base and curing agent is 10:1 so that the amount of PDMS base is chosen to be around 18 g and curing agent is 1.8 g. Slight error occurred due to manual manipulation of pouring chemicals. With the need of enough piezoelectricity output, 1.8% of $BaTiO_3$ in weight ratio is expected as discussed amount peer researchers. The amount of silver nanowires is calculated based on the percolation theory discussed in the next chapter. Thus, the amount of each chemicals is presented in the following fabrication process.

A balance is used to weigh 0.36 g of $BaTiO_3$ nanoparticles in the beaker and disperse with 25 g of ethanol. Then 2000 µL of silver nanowire suspension solution are extracted from the commercial bottle and dispense into the beaker by using the pipette dropper.

The suspension is pre-mixed using a magnetic stirring plate inside the fume hood. The spinning speed is set to 230 rpm without heating. Once the stirring process starts

and stirring bar is stable, the $BaTiO_3$ nanoparticles and silver nanowires are left for five hours until fully mixed and separated from chunks and clog.

Fig 2.1 Mixing of silver nanowires and $BaTiO_3$ nanoparticles

After the five hours of mixing, on the balance, PDMS base is poured manually by an amount of 18.89 g into the mixing beaker and put it back onto the hotplate. The hot plate is set at 55 °C and speed at 170 rpm. The process is set to continue overnight in order to let the ethanol completely evaporated form the composite mixture.

After the ethanol is completely evaporated, the heat is turned off and the stirring bar is set to continue to stir at the previously set speed to let the composite cool down to room temperature for approximately 2 hours. The mixing beaker is brought back to the balance after cooling process and add 1.89 g curing agent and put back to the magnetic stirring hotplate and continue the stirring process for another 30 minutes.

After the curing agent is fully mixed with the liquid composite, the stirring bar is picked out of the mixing beaker and 2.2 g of liquid composite is poured into the petri dish. The petri dish is then put onto a well-leveled bench top and is curing at room temperature for at least three days.

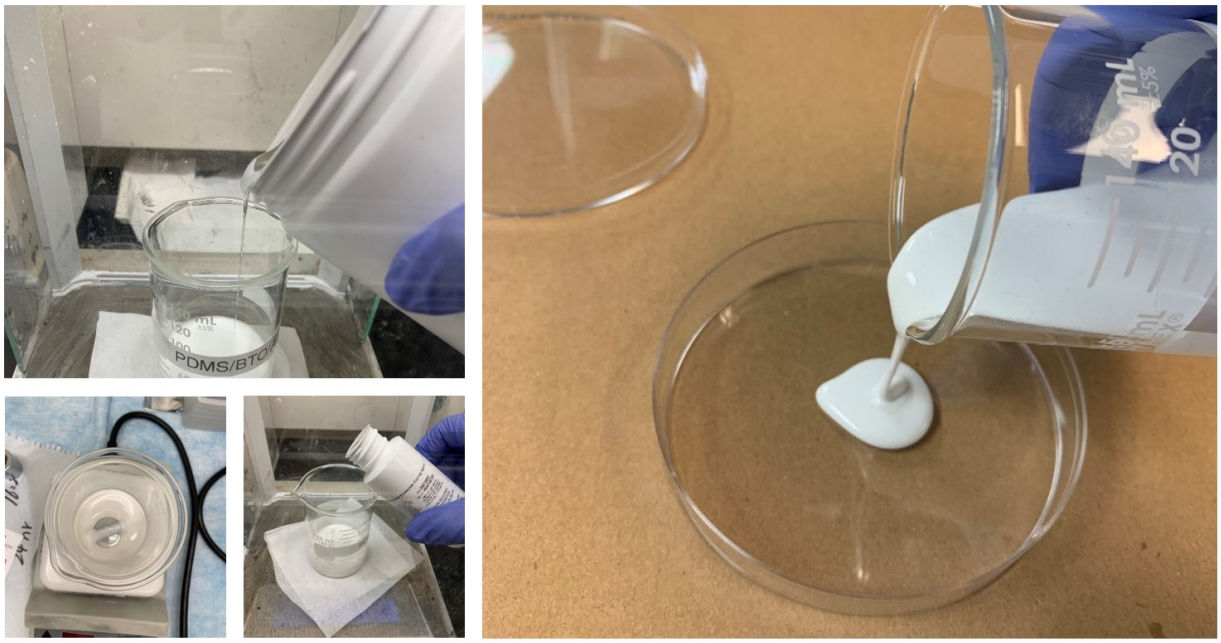

Fig 2.2 Liquid composite molding process

After the composite is cured and molded, it will form an approximately 2 mm thin film with 8 cm diameter. In this process, the thickness of piezoelectric sample is dependent on the size of the petri dish while the amount of liquid nanocomposite is greater than 2.2 g threshold. If the amount is less than 2.2 g, it won't spread out evenly due to viscosity.

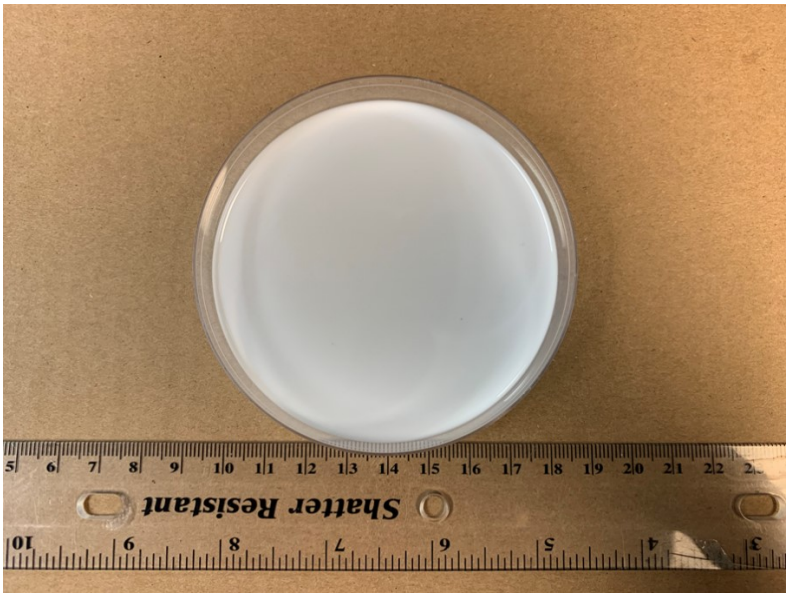

Fig 2.3 Fully cured piezoelectric nanocomposite

The translucency of well cured sample can be confirmed with unaided eye examination with a light source. Compared with nanocomposites with CNT fillers, the transmissivity of light of silver nanowires incorporated nanocomposite is better. Further experiment to accurately measure the level of translucency is expected in the future work.

2.3 Key variables and conditions

The first key condition during the process is to determine whether the ethanol is completely evaporated or not. Before adding the curing agent, one should be confirmative that the ethanol is fully evaporated by weighing the mixing beaker before and after the evaporation process. If the amount of mass lost is approximately 25 g, which is the initial amount of ethanol added, it can be confirmed that the ethanol is completely evaporated. Another key factor that significantly affect the

homogeneousness of the piezoelectric composite is the cooling process after the evaporation of ethanol. If the curing agent is added right after the heated evaporation process, the curing time will be extremely shortened due to the cross-linking mechanism affected by temperature. In order to allow ample time for liquid composite spread out evenly inside the petri dish to form a thin film, curing process must proceed under room temperature.

2.4 Chapter conclusion

In this chapter, the full fabrication process is introduced step by step from chemical preparation to the final molding process. With the continuous stirring and ethanol evaporation process, the translucent piezoelectric nanocomposite is successfully made as expected. Critical steps are discussed, and key factors and conditions are also mentioned which can cause significant problem to the whole fabrication process. This chapter provide a detailed guide for other researchers to follow when investigating similar problem or preparing similar samples.

Chapter 3

Test and Result discussion

3.1 d_{33} test and piezoelectric output

The d_{33} coefficient is one of the key constants to describe the piezoelectric behavior of a material. As mentioned in the Introduction, Fig 1.5 shows the logistic of d_{33} coefficient. Based on the direction of force applied, the frequency method is introduced when the complete matrix of the material coefficients is needed. The analyzer can collect resonance frequencies of the material to depict the piezoelectric capability.[37]

To measure the d_{33} coefficient of the fabricated composite sample, a customized set-up is introduced into the process. The shaker is not specifically designed to measure d_{33} coefficient, but it acts as an analyzer with readings of resonance frequencies. By applying certain settings, it can generate a sinusoidal wave with the adjustable amplitude loading force to measure the d_{33} output. The frequency is adjustable to accommodate different material properties.[26]

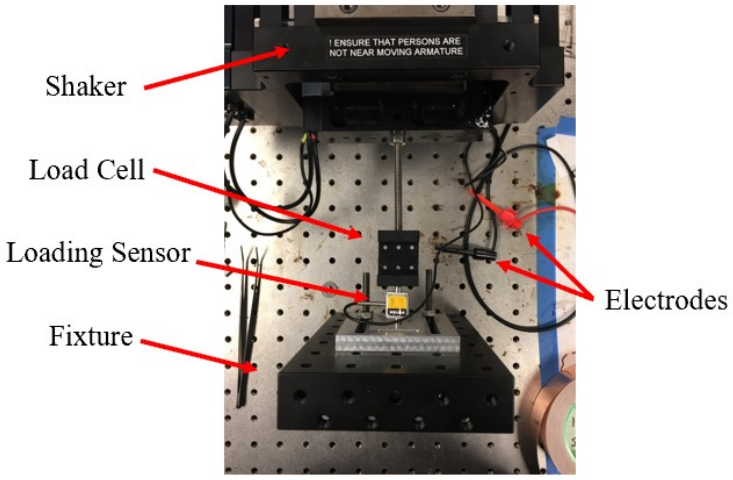

Fig 3.1 d_{33} measuring platform

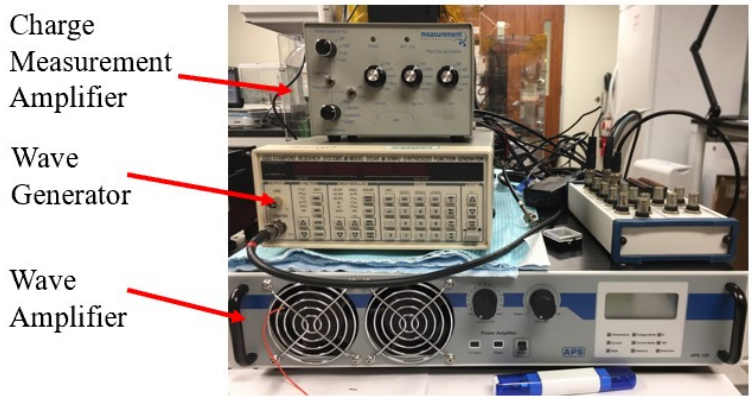

Fig 3.2 Shaker setup

The user interface is pre-programmed LabVIEW software which is a system design platform with the application of data acquisition, instrument control and industrial automation.[27]

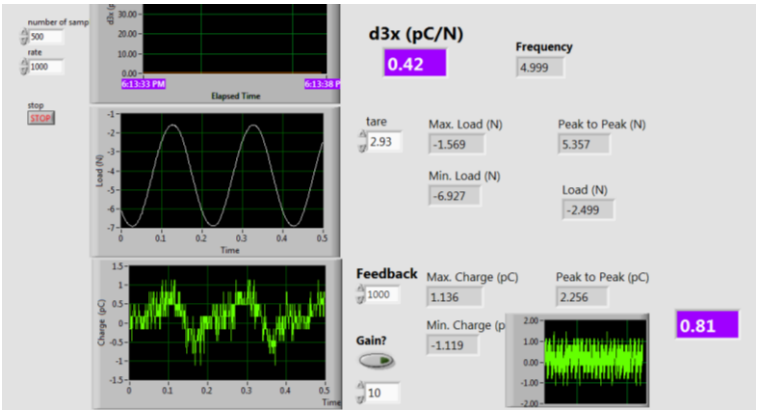

Fig 3.3 LabVIEW user interface

To start the testing process, the piezoelectric composite film inside the petri dish is cut into a 1 cm by 3 cm rectangular-shaped piece. The piece is loaded onto the testing platform in Fig 3.1. To avoid random inconsistency of the piezoelectric composite, 3 pieces of samples are cut from one single molded composite film.

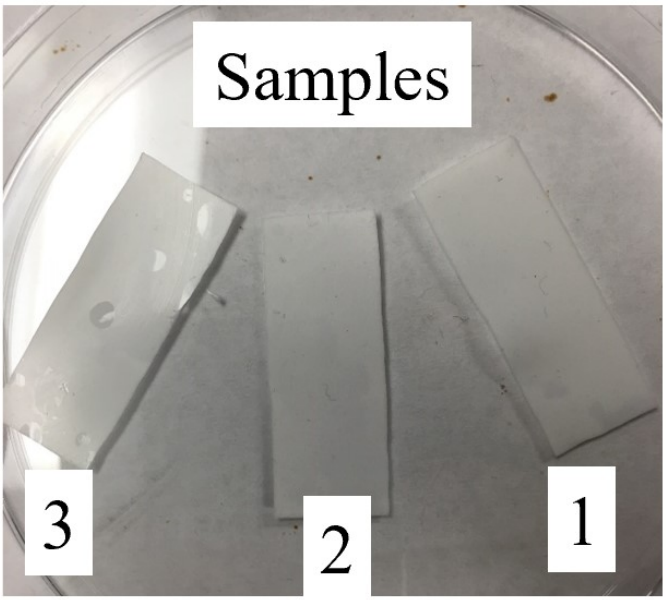

Fig 3.4 Sample prepared for testing

The frequency of the d_{33} measurement is set to 10 Hz with a compression period of 0.5 hour. The loading condition is designed with two group of loading force which are 0~5 N and 2.5 N~7.5 N. The experiments are set to compare with commercially available PVDF which is of high d_{33} coefficient.

Table 3. Loading test for d_{33} coefficient measurement

Sample	Loading Condition	
	Experiment 1	Experiment 2
1	2.5 N~7.5 N	0~5 N
2	2.5 N~7.5 N	0~5 N
3	2.5 N~7.5 N	0~5 N

After the data collection and processing, the d_{33} of each group was calculated and combined into one chart through Excel. From Fig 3.5 one can tell that has similar or even higher d_{33} coefficient and higher charges under same loading condition, compared with commercial PVDF (TE Connectivity, PN: 3-1003352-0).

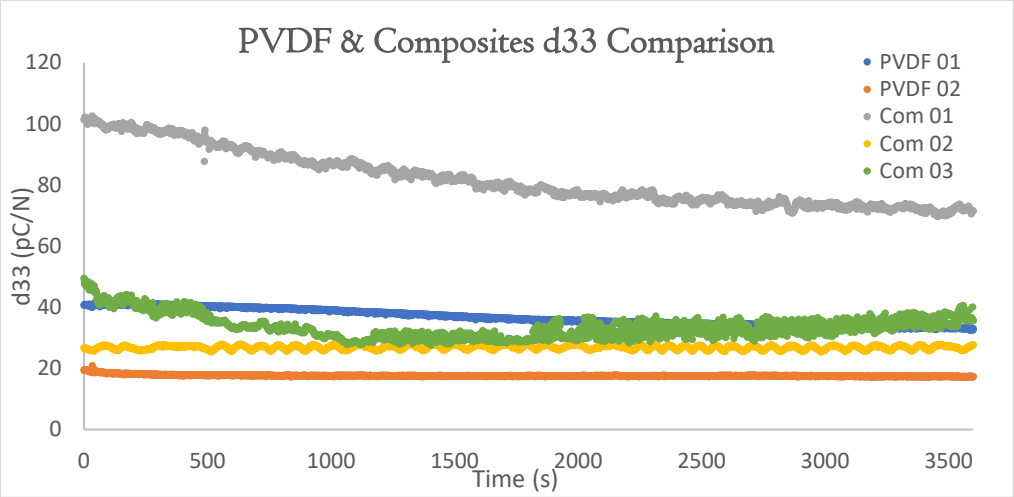

Fig 3.5 d_{33} coefficient of all testing groups under 2.5 N~ 7.5 N loading condition

The loading condition is 2.5 N~7.5N for Fig 3.5 due to the obtrusive results from the other loading condition. For the loading period of 0.5 hour, the piezoelectric composite sample 1 outperforms all other samples with the peak d_{33} measured 100 pC/N. The other two piezoelectric composite samples and the commercial PVDF fall in the same range from 20 pC/N to 50 pC/N, which is average output under the same functional materials category. As the sample 1 started at its peak, it falls gradually down to approximately 70 pC/N throughout the entire period. A lot of factors might contribute to this type of behavior such as positioning and relaxation. Even at its lowest point, the piezoelectric output still at least 50% higher than either PVDF or the other composite samples. Despite its higher output, the standard deviation as shown in Table 4., of 3 piezoelectric composites is not as small as the PVDF test groups which means the robustness of the piezoelectric composites underperforms as well.

Table 4. Standard deviation (STD) and average d_{33} values for each testing sample

	PVDF 01	PVDF 02	Com 01	Com 02	Com 03
Ave.d_{33}(pC/N)	36.7	17.7	81.6	26.9	34.2
STD (+/—)	2.7	0.3	8.9	0.6	4.0

From Table 4, there are dramatic d_{33} coefficient difference between the nanocomposite samples. Compared to commercial PVDF, which has approximately 20 pC/N, the largest difference between nanocomposite samples is 54.7 pC/N and the smallest difference is 7.3 pC/N. Such variance might indicate that there is still flaw in the fabrication process which causes the loss of uniformity. Further improvement of fabrication process is expected in the future work.

Table 5. Average d_{33} comparison between piezo nanocomposite and PVDF

Material	Piezo nanocomposites	PVDF
Ave. d_{33} (pC/N)	47.6	27.2

From Table 5, the average d_{33} coefficient of the piezoelectric nanocomposite is higher than that of PVDF by 20 pC/N, which shows the expected prediction of better performance.

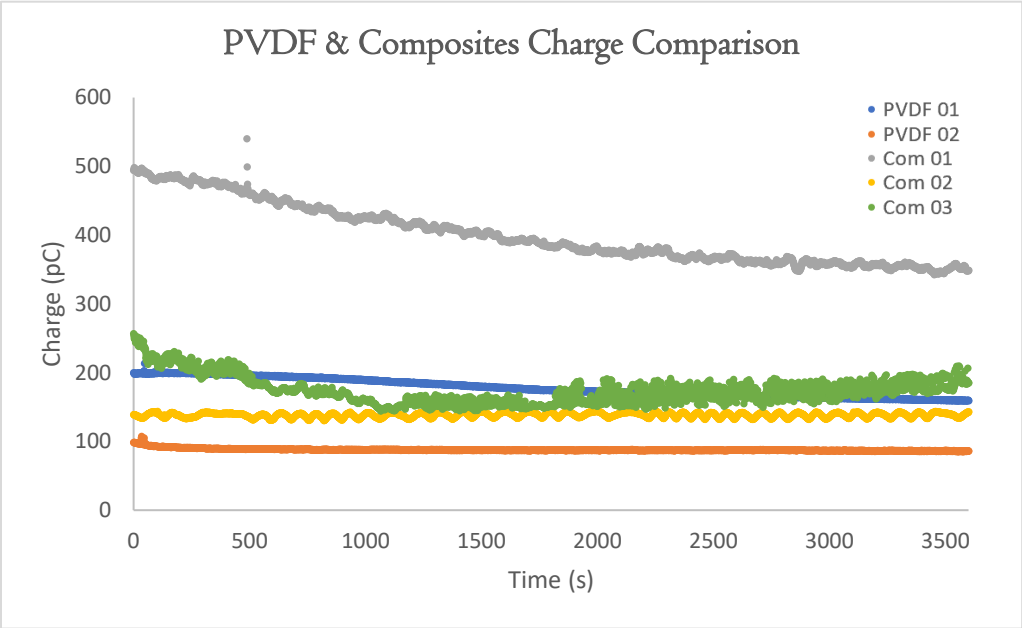

Fig 3.6 Electric charge generated from all testing group

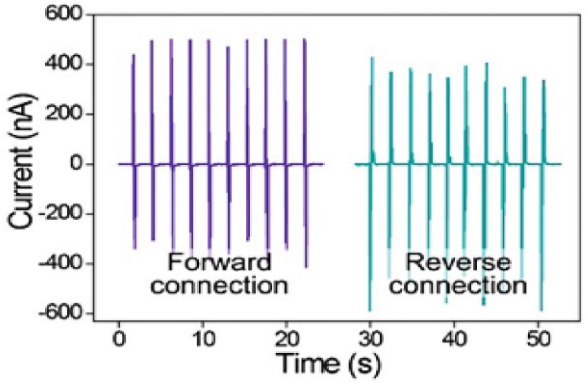

Fig 3.7 Measurement data from a previous study by Jeong et al. showing the generated outputs from periodic stretching/releasing of piezoelectric composites [20] © 2015 WILEY-VCH Verlag GmbH & Co. KGaA, Weinheim

From Fig 3.6, the charge generated from piezoelectric composite (500 pC at its peak) is higher than that that from PVDF, which is in the range of 150 ~ 200 pC. After conversed the picocoulomb to nA, the performance of piezoelectric nanocomposite is relatively the same with the peak performance of Jeong et al. [20] fabricated a bulky hyper stretchable CNT incorporated piezoelectric composite (Fig 3.7) with the stretchability of 200%.

3.2 Percolation analysis of silver nanowire network

To validate the functionality of the soft piezoelectric nanocomposite, a theoretical analysis of silver nanowire network incorporated within the composites has been carried out with the percolation theory.[28]

For a given volume of the nanowire solution (V), with a concentration of C(0.779 g/mL), the number of nanowires can be calculated by the equation

$$No.of\ silver\ nanowires = \frac{4CV}{D_{Ag}\pi d^2 L} \qquad Eq.(1)^{[28]}$$

where D_{Ag} is the density of bulk silver (10.5 g/mL), d is the average diameter (135 nm), and L is the average length (35 μm) of the Ag nanowire provided by the supplier. After molding, these nanowires were assumed evenly distributed inside the PDMS matrix on the petri dish of 87 mm diameter (D). Hence, the density of nanowires, N

can be calculated by dividing the number of nanowires by the area of the petri dish, and is given by

$$N = \frac{4CV}{D_{Ag}\pi d^2 L}/\pi D^2/4 \qquad eq.(2)^{[28]}$$

Substituting the corresponding values in the above equation gives $N = 0.24364\,V$• μm^{-2} for a given volume (V) of the nanowire solution used. According to the standard percolation theory, the density dependence of conductivity is given by

$$\sigma \propto (N - N_C)^{\alpha} \qquad eq.(3)^{[28]}$$

where σ is the conductivity in three dimensions, or sheet conductance in two dimensions, N_C is the critical nanowire density required for the onset of conduction in a random network, and α is a critical exponent which depends on the dimensionality of the space involved. The theoretical values of α are 1.33 for a 2-D percolation network and 1.94 for a 3-D percolation network.[29]

For a 2-D network, the sheet resistance (R_{sh}) is given by R_{sh} = 1/sheet conductance, and the relation between R_{sh} and volume (V) of the nanowire solution can be obtained using equation as follows

$$R_{sh} \propto (V - V_c)^{-\alpha} \qquad eq.(4)^{[28]}$$

Fig 3.8 shows the variation of sheet resistance with the volume of nanowire solution used and the solid line represent the fitted curve obtained using equation above. In order to obtain the fitting curve, the value of V_c as 0.20 mL was taken as this was the minimum volume required to achieve a conducting film.

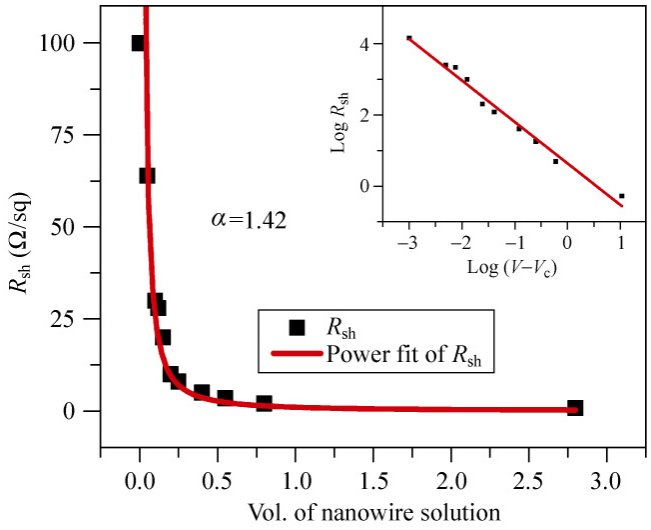

Fig 3.8 Plot of sheet resistance versus volume of Ag nanowire solution; reproduced with permission from [28] © 2010 Springer

Based on calculations performed above, one is able to speculate that with the use of 2000 μL in total, which is 0.33 mL per sample, of silver nanowires solution, it is sufficient to create conductive random network within the fabricated soft piezoelectric nanocomposite.

3.4 Chapter conclusion

In this chapter, the piezoelectric output test was introduced and explained step by step. The result shows the outperformance of silver nanowire incorporated soft piezoelectric nanocomposite. A comparison was made with similar composite material. An analysis of the percolation of silver nanowires was conducted through mathematic models and validation of functionality was testified. The application of soft

piezoelectric nanocomposite in diagnosis and robotics was also introduced in this chapter.

Chapter 4

Conclusion and future work

4.1 Conclusion

In this essay, the synthesis and measurements of silver nanowire-based piezoelectric composites are introduced for improvement of transparency while maintaining high piezoelectric output. The fabrication process of soft piezoelectric nanocomposite was explained step by step. Testing method and results are reported.

The fabricated nanocomposites showed promising results with higher d_{33} piezoelectric coefficients, which averages 47.60, than commercial piezoelectric polymer PVDF, which averages 27.19. Moreover, compared with other piezoelectric composites, the synthesized materials showed enhanced light transmission, making it attractive for a wider range of applications.

4.2 Future work

To increase the consistency of piezoelectric output, the fabrication process still needs to be modified. Iteration of controlled variable experiment need to be carried out to leave out detrimental factors, such as cooling of liquid composite and evaporation calculation, that decrease the performance capability of piezoelectric composite. Improvements of fabrication process need to be done in order to provide consistency of sample piezoelectric output. Further discussion of mixing ratio of the chemicals also needs to be carried out. The transmissivity of the composite has not been tested qualitatively and quantitively by certain method such as a transmittance meter. Further proof of better performance needs to be collected through comparison with other piezoelectric nanocomposites.

Bibliography

[1]. Antonio Arnau, “Fundamentals of piezoelectricity.” Piezoelectric transducers and applications, 2008

[2]. Gautschi, G. Piezoelectric Sensorics: Force, Strain, Pressure, Acceleration and Acoustic Emission Sensors, Materials and Amplifiers. Springer, 2002

[3]. Krautkrämer, J. & Krautkrämer, H. Ultrasonic Testing of Materials. Springer, 1990

[4]. Jaffe, B.; Cook, W. R.; Jaffe, H. Piezoelectric Ceramics. New York: Academic, 1971

[5]. Sappati, Kiran; Bhadra, Sharmistha; Sappati, Kiran Kumar; Bhadra, Sharmistha. "Piezoelectric Polymer and Paper Substrates: A Review". Sensors. 2018

[6]. Heywang, Walter; Lubitz, Karl; Wersing, Wolfram, eds. Piezoelectricity: evolution and future of a technology. 2008

[7]. Soin, N.; Boyer, D.; Prashanthi, K.; Sharma, S.; Narasimulu, A.; Luo, J.; Shah, T.; Siores, E.; Thundat, T.Exclusive self-aligned b-phase PVDF films with abnormal piezoelectric coefficient prepared via phase inversion. Chem. Commun. 51, 8257–8260, 2015

[8]. Sappati, Kiran; Bhadra, Sharmistha; Sappati, Kiran Kumar; Bhadra, Sharmistha. "Piezoelectric Polymer and Paper Substrates: A Review". Sensors. 18 (11): 3605, 2018

[9]. Harrison, J.; Ounaies, Z.; Bushnell, D.M. Piezoelectric Polymers; NASA Langley Research Center: Hampton, VA, USA, 2001.

[10]. G. Schwartz, B. C. Tee, J. Mei, A. L. Appleton, H. Kim do, H. Wang and Z. Bao, Nat. Commun., 4, 1859, 2013

[11]. Jing, Q., Xie, Y., Zhu, G., Han, R. P. S. & Wang, Z. L. Self-powered thin-film motion vector sensor. Nat. Commun. 6, 8031, 2015

[12]. Smith, W.A. The role of piezocomposites in ultrasonic transducers. In Proceedings of the Ultrasonics Symposium, Montreal, QC, Canada, 3–6; pp. 755–766,1989

[13]. Jing, Li, et.al., Analytical, numerical, and experimental studies of viscoelastic effects on the performance of soft piezoelectric nanocomposites. Nanoscale, 9, 14215, 2017

[14]. T. Ikeda, Piezoelectricity, Oxford University Press 1990

[15]. Ferry, D. K. Nanowires in Nanoelectronics. Science, 319 (5863), 579–580, 2008

[16]. Jin Hwan Lee et al., Large-Scale Synthesis and Characterization of Very Long Silver Nanowires via Successive Multistep Growth, Cryst. Growth Des.,12, 5598–5605, 2012

[17]. Marks, T. J.; Janes, D. B. Fabrication of Fully Transparent Nanowire Transistors for Transparent and Flexible Electronics. Nat. Nanotechnol., 2 (6), 378–384, 2007

[18]. Park, Kwi-Il, et al. "Stretchable piezoelectric nanocomposite generator." Nano Convergence 3.1, 1-12, 2016

[19]. K.-I. Park, M. Lee, Y. Liu, S. Moon, G.T. Hwang, G. Zhu, J.E. Kim, S.O. Kim, D.K. Kim, Z.L. Wang, K.J. Lee, Flexible nanocomposite generator made of $BaTiO_3$ nanoparticles and graphitic carbons. Adv. Mater. 24(22), 2999–3004, 2012

[20]. C.K. Jeong, J. Lee, S. Han, J. Ryu, G.-T. Hwang, D.Y. Park, J.H. Park, S.S. Lee, M. Byun, S.H. Ko, K.J. Lee, A hyper-stretchable elastic-composite energy harvester. Adv. Mater. 27(18), 2866–2875, 2015

[21]. Peng Jiang, et al., Machinable Long PVP-Stabilized Silver Nanowires, Chem. Eur. J., 10, 4817 – 4821, 2004

[22]. Hyungseok Kang, et al., Mechanically robust silver nanowires network for triboelectric nanogenerators, Adv. Funct. Mater., 26, 7717–7724, 2016

[23]. Yue Shi, et al., Synthesis and Applications of Silver Nanowires for Transparent Conductive Films, Micromachines, 10, 330, 2019

[24]. Jing Li, et al., Ultrasensitive, flexible, and low-cost nanoporous piezoresistive composites for tactile pressure sensing, Nanoscale, 11, 2779, 2019

[25]. Shah, Jyoti & Kotnala, R.K., Induced magnetism and magnetoelectric coupling in ferroelectric $BaTiO_3$ by Cr-doping synthesized by a facile chemical route. J. Mater. Chem. 2013

[26]. Decheng Hou, Bioinspired Composite Self-Stiffening in Response to External Stress, 2018

[27]. Bress, Thomas J. Effective LabVIEW Programming. [S.l.]: NTS Press. 2013

[28]. Anuj R. Madariaet et al., Uniform, Highly Conductive, and Patterned Transparent Films of a Percolating Silver Nanowire Network on Rigid and Flexible Substrates Using a Dry Transfer Technique, Nano Res, 3: 564–573, 2010

[29]. Stauffer, G. Introduction to Percolation Theory; Taylor & Francis: London, 1985

[30]. Seong Kyu Cheon, Min Ho Park, Seong Su Jeong, Ho Ik Jun, Tae Hoon Kim & Tae Gone Park, Development of small robot using piezoelectric benders, Integrated Ferroelectrics, 195:1, 81-90, 2019

[31]. S. Avadhanula, "Design, fabrication and control of the micromechanical filying insect", U.C, Berkeley, 2006

[32]. Shannon A. Rios, Andrew J. Fleming, and Yuen Kuan Yong, Miniature Resonant Ambulatory Robot, IEEE Robotics and Automation Letters, VOL. 2, NO. 1, 2017

[33]. C.-H. Rhee, J. S. Pulskamp, R. G. Polcawich, and K. R. Oldham, "Multi-degree-of-freedom thin-film PZT-actuated microrobotic leg," J. Microelectromechanical Syst., vol. 21, no. 6, pp. 1492–1503, 2012

[34]. Ehsaneh Shahhaidar, Bryson Padasdao, R. Romine, C. Stickley and Olga Boric-Lubecke, Piezoelectric and Electromagnetic Respiratory Effort Energy Harvesters, 35th Annual International Conference of the IEEE EMBS, 2013

[35]. Bin He and Zhanjie Wang, Enhancement of the Electrical Properties in $BaTiO_3/PbZr_{0.52}Ti_{0.48}O_3$ Ferroelectric Superlattices, ACS Appl. Mater. Interfaces, 8, 6736−6742, 2016

[36]. Tzeno Galchev, Ethem E. Aktakka, Hanseup Kim and Khalil Najafi, A Piezoelectric Frequency-increased Power Generator for Scavenging Low-Frequency Ambient Vibration, IEEE 23rd International Conference on Micro Electro Mechanical Systems (MEMS), 2010

[37]. Fialka, J, Determination of the Tiezoelectric Charge Constant d_{33} Measured by the Laser Interferometer and Frequency Method, DAAAM Symposium, Volume 21, No. 1, 2010

Vita

Shichen Xu was born in Baoding, Hebei, China on October 20th, 1992. He received his bachelor's degree in Mechanical Engineering from Purdue University. He then enrolled in the M.S.E. program of Mechanical Engineering at Johns Hopkins University in 2017 and will move to Minnesota to work for Access Point Technologies EP as mechanical design engineer starting winter 2019.